Journal of Applied Sciences

ISSN 1812-5654

science alert

ANSInet
an open access publisher
http://ansinet.com

Journal of Applied Sciences 10 (12): 1028-1035, 2010
ISSN 1812-5654

Pure and La-Doped SnO_2 Catalytic Pellet by Using Sol-Gel Method for Ethanol Vapour Detection

X.J. Tan, G.W. Lim, G.T. Ang and M.Z. Abu Bakar
School of Chemical Engineering, Engineering Campus, Universiti Sains Malaysia,
Seri Ampangan, 14300 Nibong Tebal, Pulau Pinang, Malaysia

Abstract: This study describes the development of pure and lanthanum doped tin dioxide catalytic pellets in detecting ethanol vapour prepared by sol-gel method and pressed into pellet. Sintering treatment at 500°C was carried out for 4 h. Structural characterization was performed using X-Ray Diffraction (XRD), Transmission Electronic Microscopy (TEM) and BET surface area analyzer. The results of structural analysis showed that lanthanum has been successfully incorporated into the SnO_2 crystal lattice. The catalytic pellets gas sensing performance revealed that the sensitivity of the sensor is improved by the addition of lanthanum. The linear dependence of the sensitivity on the ethanol vapour concentration is observed in the range of 800-3000 ppm. The maximum sensitivity is exhibited by 10 at. % La-SnO_2 catalytic pellet at operating temperature of 300°C. The response and recovery time are increased by introduction of lanthanum into tin oxide. Pure SnO_2 catalytic pellet gives the fastest response and recovery time which are 22.8 sec and 4.1 min, respectively.

Key words: Sol gel, La-SnO_2, ethanol, catalytic sensor

INTRODUCTION

Semiconductor metal oxide gas sensors such as ZnO, SnO_2, WO_3, TiO_2, α-Fe_2O_3 and etc. have been proven to be very promising at monitoring the emission of dangerous gases into the atmosphere (Labidi *et al*., 2006). Of all the metal oxides that have gas-sensing behaviour, SnO_2-based sensor material has been widely studied for gas sensing applications. Other applications of SnO_2 include optoelectronic devices, dye-base solar cells, secondary lithium batteries electrode materials and catalysts (Fang *et al*., 2008). Besides, SnO_2 is preferred by most researchers since it offers low cost, simple design, fast response and low power consumption.

Many researches have focused on SnO_2 based gas sensors for detection of ethanol vapours previously due to its promising properties (Hyodo *et al*., 2003; Wang *et al*., 2006; Ge *et al*., 2006; Caihong *et al*., 2007). However, the drawback of SnO_2 sensors is that gas sensing properties of pure tin dioxide suffer from high operating temperature and poor selectivity towards similar reducing gases, which limit its applicability in real-time gas sensing devices (Rani *et al*., 2007). In order to achieve better sensitivity and selectivity of with SnO_2-based sensors, different techniques have been applied such as optimizing the doping, the operating temperature, or the substrate geometry (Khodadadi *et al*., 2001). Among these, doping method is chosen. For this purpose, lanthanum is selected as the catalytically active material because it has been reported to be a promising promoter for SnO_2-based ethanol vapour sensors by the researchers (Stambolova *et al*., 2000; Zhu *et al*., 2004) through modification in sensing material's structure and morphology (Kapse *et al*., 2009).

Although the study of La-doped SnO_2 on detection of ethanol vapour has been carried out by several researchers (Jinkawa *et al*., 2000; Weber *et al*., 2008; Hieu *et al*., 2008), there is no study on the gas sensing characteristics of catalytic pellet sensor. Hence, in this study, La-SnO_2 catalytic pellet using sol-gel method will be developed and the structural as well as gas sensing characteristics will be studied.

MATERIALS AND METHODS

Pellet sensor fabrication: The La-SnO_2 powder is prepared through a sol-gel route which is as follows: tin tetrachloride pentahydrate lump ($SnCl_4.5H_2O$) was first dissolved in 50 mL of ethanol solution (ethanol and de-ionized water with volume ratio 1:1) to a concentration of 2 M. The solution was stirred vigorously for about 20 min until a transparent sol was produced. In order to study the effect of La dopant in the sensing performance, lanthanum nitrate hexahydrate ($La(NO_3)_3.6H_2O$) was added

Corresponding Author: X.J. Tan, School of Chemical Engineering, Engineering Campus, Universiti Sains Malaysia, Seri Ampangan, 14300 Nibong Tebal, Pulau Pinang, Malaysia

Table 1: Quantity of chemicals needed to produce powder

Quantity	Pure SnO_2	5% La-SnO_2	10% La-SnO_2
Concentration of $SnCl_4.5H_2O$ (mol L^{-1})	2.00	2.00	2.00
Volume of ethanol solution (mL)	50.00	50.00	50.00
Molecular weight of $SnCl_4.5H_2O$ (g mol^{-1})	350.58	350.58	350.58
Mass of $SnCl_4.5H_2O$ (g)	35.06	35.06	35.06
Mole of Sn in solution (mol)	0.10	0.10	0.10
Ratio of Sn	1.00	0.95	0.90
Ratio of La	0.00	0.05	0.10
Mole of La in solution (mol)	0.00	0.005	0.011
Molecular weight of $La(NO_3)_3.6H_2O$ (g moL^{-1})	433.01	433.01	433.01
Mass of $La(NO_3)_3.6H_2O$ (g)	0.00	2.28	4.81

to the solution and stirred for 30 min at 80°C. The atomic ratio of La to Sn was 5:95 and 10:90. Ammonia solution was added slowly to the mixture until gellification of the sol yielded. After 48 h of aging in the air, the SnO_2 gel was centrifuged with a centrifugal machine (Eppendorf 5804R) at 3000 rpm for 5 min and the solid gel was collected. The solid gel was centrifuged in de-ionized water repeatedly for 5 times in order to remove the ammonia, chloride and nitrate components. The amount of chemicals needed for production of powder is shown in Table 1. The collected gel was then dried in an oven at 80°C for 4 h to remove the moisture. Afterwards, the dried gel was sintered at 500°C for 4 h in a furnace (carbolite ELF 11/63). The sintered powder was crashed and sieved with a 75 micron sieve. The powders were then cool pressed into pellets. Finally, the pellets were sintered again at 500°C.

Morphological and structural characterization: XRD was used to identify structure and determine the crystalinity of the catalytic pellets. In this study, XRD patterns of the pellets were obtained using an X-ray diffractometer (Philips PW 1710) with a Cu K_α X-ray source of 1.5418 Å. The analysis was performed at room temperature (25°C) over 2 theta range of 10°-90° with a step size of 0.034° and a step time of 35.8 sec.

The surface morphology of the powder was examined with TEM images which were snapped with Philips CM12 transmission electron microscope that operated at 80 kV. The sample must be deposited on a copper grid before transferring into the transmission electron microscope. It was begun by suspending a small quantity of powder sample in absolute ethanol liquid. The sample was shake and left for settling. A drop of ethanol containing the lightest powder sample was deposited on a carbon film coated 400 mesh copper grid for 2 min. The remaining solution on the grid was wiped carefully with a filter paper. Finally the grid was sent for image snapping.

The Brunauer, Emmett and Teller (BET) surface area of the sample powders were measured by nitrogen adsorption at 77 K using surface area and porosity analyzer (Micromeritics ASAP 2020). All samples were degassed by using nitrogen at 350°C for 4 h prior to analysis.

Gas sensing measurements: The gas sensing performance of developed pellets was tested by a testing chamber. In the chamber, the catalytic pellet sensor was slotted between two silver clippers which were connected to electrometer (Keithley 6517A) with the applied voltage range of 5 V. The ethanol was vapourized in a water bath at a constant temperature of 40°C. The heater in the gas chamber was set at desired working temperature range from 150 to 300°C. Then air was mixed with different ethanol vapour flows in which flowrates were regulated and measured by mass flow controllers to achieve desired ethanol vapour concentrations range from 800 to 3000 ppm. Prior to testing, the concentrations of ethanol vapour were analyzed and calibrated using a gas chromatography (Hawlett Packard, 5890 series II) connected to a Porapak Q column with dimension of 3 m length × 2.33 mm ID. Helium was used as carrier gas. During the gas sensor measurement testing, 300 mL min^{-1} of air was initially flowed into the chamber for 200 sec and then followed by 300 sec of the mixed air and ethanol vapour flow. Then, the chamber was flowed with air again for 200 sec. All the dc resistance of pellet sensor was measured for each second using the electrometer. A computer equipped with LabVIEW software via a GPIB interface was used for data acquisition, storage and plotting in real time for the analysis of sensitivity of gas sensor.

RESULTS AND DISCUSSION

XRD analyses: XRD was used to identify the phases and to evaluate the crystallite sizes of the pellets as a function of La concentration. Figure 1a-c display the XRD patterns of pure SnO_2 and La-doped SnO_2. XRD patterns are indexed with SnO_2 with tetragonal structure (ICCD Card No. 01-088-0287), which is the main phase. From Fig. 1b and c, the peaks corresponding to any intermediate compound or pure La_2O_3 are not observed, indicating the formation of a solid solution between SnO_2 and La_2O_3 within the concentration of doping by the sol-gel technique (Kapse *et al*., 2009). Figure 1 also shows that all samples have the sharp diffraction peaks indicate the as-received samples have a high degree of crystallization.

The crystallite size, D with respect to La-dopants concentration is calculated using Scherrer's equation, provided in Eq. 1 (Kapse *et al*., 2009).

$$D = \frac{K\lambda}{B\cos\theta} \quad (1)$$

where, K is a constant which depends on the line shape profile, λ is the wavelength of the x-ray source and B is

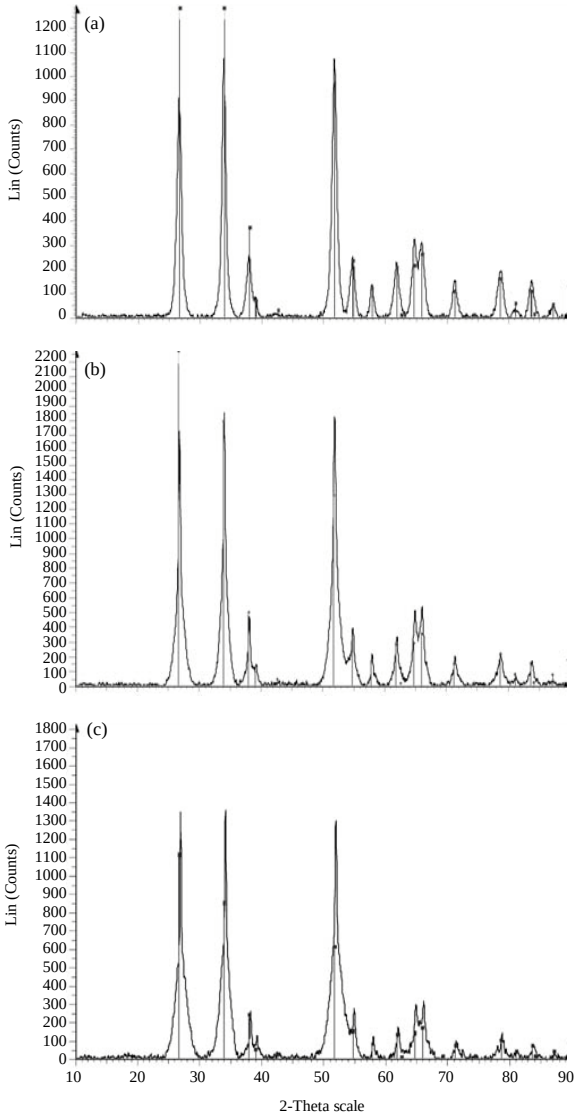

Fig. 1: X-ray diffraction patterns of pellets with pure SnO_2 and different La contents. (a) Pure SnO_2 (b) 5 at.% La-doped SnO_2 and (c) 10 at.% La-doped SnO_2

the full width at half maximum intensity (in radians) of a peak at an angle θ. The calculated values of SnO_2 phase are shown in Table 2.

The results shown in Table 2 indicate that smaller and less ordered crystals are formed in the case La-doped samples. The crystallite size decreases with the increasing of atomic ratio lanthanum dopants. This indicates that high dopant concentrations may lead to supersaturation which is responsible for hindering grain growth (Weber *et al*., 2008). From the effect of lanthanum dopants

Table 2: Crystallite size calculated using Scherrer's equation

	Crystallite size (nm)		
	Pure SnO_2	5 at.% La	10 at.% La
Tetragonal SnO_2	14.37	6.64	3.52

Table 3: BET surface area for pure and La-doped SnO_2 samples

	Pure SnO_2	5 at.% La	10 at.% La
BET surface area (m^2 g^{-1})	45.88	92.73	95.16

on crystallite sizes, again, we can consider that it is reasonable that the added La^{3+} has been successfully incorporated into the crystal structure of SnO_2 although the peaks associated with La^{3+} cannot be observed from Fig. 1b and c. On the other hand, it is desirable that the sensor material has smaller size to attain high sensitivity to gases (Lee *et al*., 2000).

TEM analyses: The morphology of powders was examined with TEM and the images of pure, 5 at.% La-doped and 10 at.% La-doped SnO_2 powders are shown in Fig. 2a-c, respectively. There is a noticeable reduction in average tetragonal particle size of SnO_2 when lanthanum is doped onto the SnO_2. From the TEM images, for pure SnO_2, the size of the crystallites is about 8.9 nm. The size decreases to 5.5 and 4.0 nm for SnO_2 doping with 5 at.% La and 10 at.% La, respectively. The average crystallite size estimated from XRD corroborates with the TEM investigation. In addition, a significant amount of agglomeration was observed in the micrographs especially for sample powder of 10 at.% La-doped SnO_2.

BET surface area analyses: Measurements of surface area of the powders were carried out with standard Brunnauer-Emmett-Teller (BET) surface area analyzer and the values are displayed in Table 3. It was observed that addition of dopant caused the doped system to show higher surface area which is about 2.0 times larger than the pure system. This effect is more significant when larger amount of dopant is added. It is clear that the addition of lanthanum makes the SnO_2 more porous. The smaller particle size as observed by XRD, also supports high surface area of the doped powder (Rella *et al*., 1997). Higher surface area is required for gas sensor to enhance the catalytic performance and hence the sensitivity of the sensor.

Effect of temperature on sensing properties: Figure 3 shows the plot of resistance versus time for 10 at.% La-doped SnO_2 sensor which was tested under 150°C. The sensor was exposed to pure air from time 0 to 200 sec, followed by 1500 ppm of ethanol vapour until 500 sec. The average electrical resistance of sensor at pure air

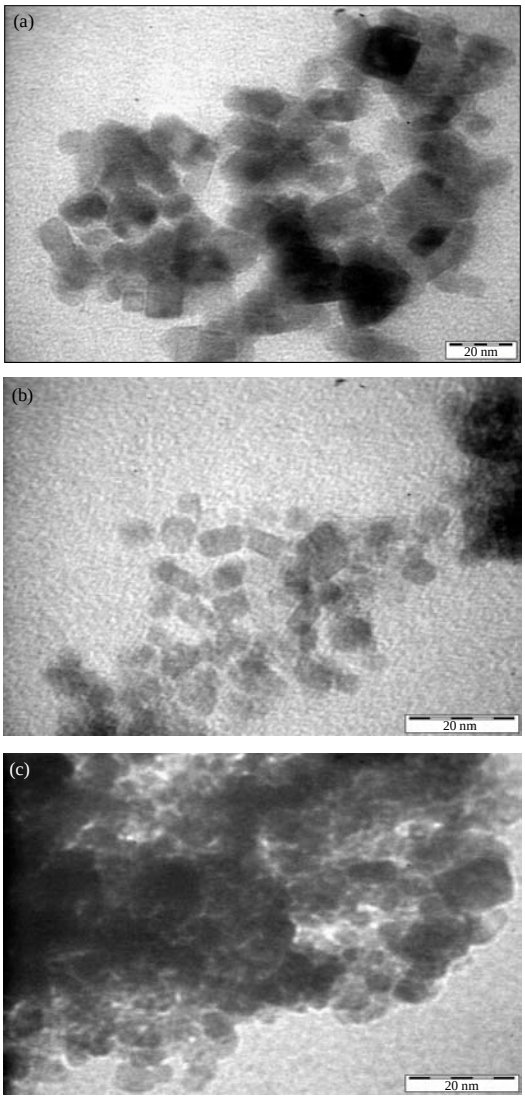

Fig. 2: Transmission electron microscopic images of pure and La-doped SnO_2 samples. (a) Pure SnO_2, (b) 5 at.% La-doped SnO_2 and (c) 10 at.% La-doped SnO_2

atmosphere, R_a and average electrical resistance of sensor at ethanol vapour atmosphere, R_g were obtained and sensitivity, S was calculated according to the Eq. 2 (Ruis *et al*., 2004):

$$S = \frac{R_a}{R_g} \quad (2)$$

The response transient for other samples at different conditions behaved the same as that shown in Fig. 3.

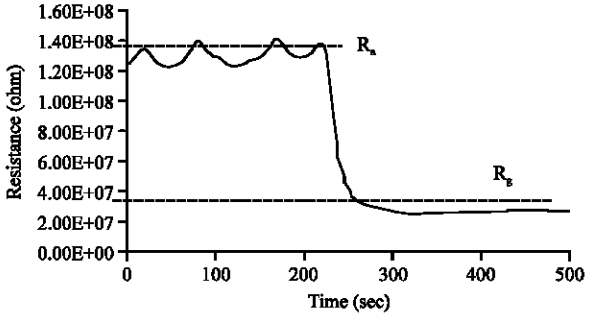

Fig. 3: Plot of resistance versus temperature for 10 at.% La-doped SnO_2 sensor at 150°C

The gas-sensing mechanism of SnO_2 based sensors belongs to the surface-controlled type, that is, the resistance change is controlled by the species and amount of chemisorbed oxygen on the surface (Kapse *et al*., 2009). When pure air passes through the gas sensor, O_2 is adsorbed on the sensor surface. It traps electrons from the conduction band of the sensors material to produce negatively charged chemisorbed oxygen such as O_2^-, O^- and O^{2-} which create a depletion layer at the surface of the individual particles and inter-granular regions. Consequently, the concentration of electrons in the n-type SnO_2 decreases and hence the resistance of the material increases. The process can be expressed by Eq. 3-6 (Chang *et al*., 2002):

$$O_2(gas) \leftrightarrow O_2(ads) \quad (3)$$

$$O_2(ads) + e^- \leftrightarrow O_2^-(ads) \quad (4)$$

$$O_2^-(ads) + e^- \leftrightarrow 2O^-(ads) \quad (5)$$

$$O^-(ads) + e^- \leftrightarrow O^{2-}(ads) \quad (6)$$

When the SnO_2 based sensor is exposed to the ethanol vapour, the surface adsorbs the vapour and interaction of ethanol vapour with the surface chemisorbed oxygen, which exists in various forms can take place in different ways of reaction. The ethanol vapour is an electron donor and hence releases electrons back to the conduction band through oxidation reaction with the surface chemisorbed oxygen (Zhu *et al*., 2006; Mardare *et al*., 2008; Kapse *et al*., 2009). Thus, the electrical conductance of the semiconductor increases. This can be observed from Fig. 3 in which the resistance drops tremendously once ethanol vapour is introduced to the system.

The sensitivity variation of undoped and lanthanum doped SnO_2 gas sensors as a function of operating temperature (150-350°C) and ethanol vapour

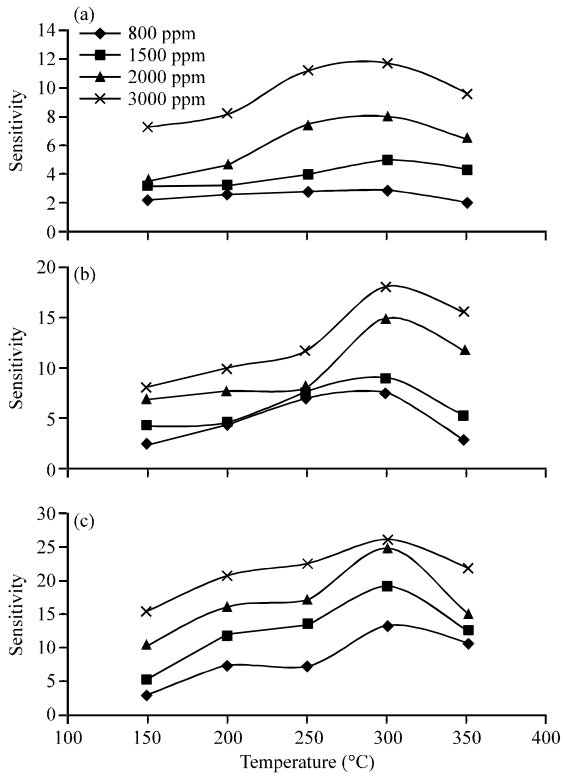

Fig. 4: Sensitivity variation of pure and La-doped SnO_2 sensors at various operating temperatures and ethanol vapour concentrations. (a) Pure SnO_2, (b) 5 at.% La-doped SnO_2 and (c) 10 at.% La-doped SnO_2

concentration (800-3000 ppm) is displayed in Fig. 4a-c. It can be observed that maximum sensitivity is achieved under exposure to 3000 ppm of ethanol vapour at 300°C for all the pure and La-doped SnO_2 sensors. For pure SnO_2 sensor, the maximum sensitivity is 11.68 whereas for 5 at.% and 10 at.% La-doped SnO_2 sensor, maximum sensitivity are 18.06 and 26, respectively.

Figure 5 shows the sensitivity variation of undoped and lanthanum doped SnO_2 gas sensors as a function of operating temperature (150-350°C) towards 1500 ppm ethanol vapour. From Fig. 3, the sensitivity increases with an increase in the operating temperature, reaching a maximum value corresponding to an optimum operating temperature which is 300°C for all undoped and lanthanum doped SnO_2 samples. Further increasing the temperature over 300°C, however, caused ethanol sensitivity to decrease again. The increase in sensitivity with operating temperature can be attributed to the fact that the thermal energy obtained was high enough to overcome the activation energy barrier of the reaction, while the reduction in sensitivity was due to the difficulty in

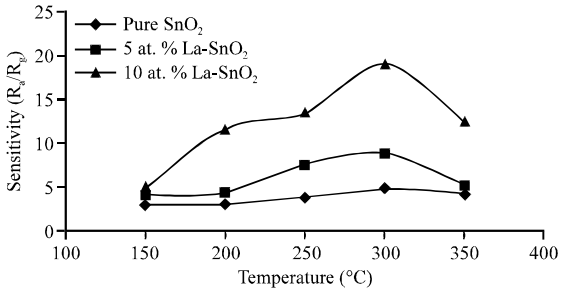

Fig. 5: Sensitivity variation of pure and La-doped SnO_2 sensors at various operating temperature towards 1500 ppm of ethanol vapour

exothermic vapour adsorption (Chang *et al*., 2002). Besides, it is evident that the introduction of lanthanum leads to an increase in ethanol sensitivity, the best properties being observed with 10 at.% La-doped SnO_2 which gives an optimum sensitivity of 19.06. At lower lanthanum content, the sensitivity is close to that of undoped system at low temperature which is below 200°C. The maximum sensitivity of pure SnO_2 and 5 at.% La-doped SnO_2 are 9.01 and 4.96, respectively.

Basically, there are two types of reactions can be occurred during interaction of ethanol vapour with the chemisorbed oxygen on the surface of the sensors and the selectivity of the reaction is known to be influenced by acid base properties on the oxide surface. The reaction that occurs on basic surface is referred to dehydrogenation and is presented as follow (Stambolova *et al*., 2000; Rani *et al*., 2007):

$$C_2H_5OH \rightarrow CH_3CHO + H_2 \quad (7)$$

Dehydrated of ethanol to C_2H_4 is favored on the acidic surface through the reaction below:

$$C_2H_5OH \rightarrow C_2H_4 + H_2O \quad (8)$$

During the reaction between ethanol and chemisorbed oxygen, CH_3CHO produced from Eq. 7 is known to have much higher molecular sensitivity to a semiconductor gas sensor than C_2H_4. Lanthanum oxide which is an basic oxide is introduced in SnO_2 matrix promotes the basicity of the surface and causes the dehydrogenation to be more favored than dehydration. Consequently the ethanol sensitivity is increased (Stambolova *et al*., 2000). The improvement of sensitivity can also be explained by the decreasing of crystalline size when the La dopant concentration rises. As crystallite size decreases, the surface to volume ratio increases largely leads to better sensitivity (Lou *et al*., 2007). Hence,

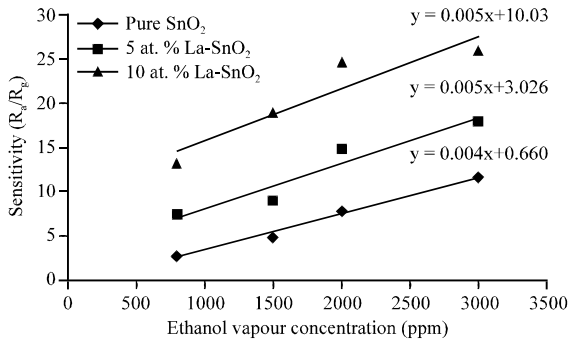

Fig. 6: Dependence of sensor response on ethanol vapour concentration at the operating temperature 300°C for pure and La-doped SnO_2 sensors

it is evident that 10 at.% La-doped SnO_2 gas sensor which has the highest lanthanum content, smallest crystallite size and largest surface area exhibited the highest sensitivity towards ethanol vapour.

Effect of ethanol vapour concentration: Figure 6 displays the sensitivity of sensors with the variation of ethanol vapour concentration at optimal operating temperature of 300°C and linear calibration curves are observed. This is because at a fixed specific surface coverage of area, a high gas concentration implies a high coverage of gas molecules. Hence, this leads to higher interaction between the gas and material surface and thus the higher sensitivity. Besides, the sensitivity is also improved by the addition of lanthanum as dopant. This confirms that the La-doped SnO_2 pellets can be used as a promising material for ethanol sensors.

Moreover, the sensitivity of metal oxide is usually defined as $S= A[C]^N+B$ where A and B are constants and [C] is the concentration of the target ethanol vapour. Sensitivity increases linearly with ethanol concentration, hence N=1.0 for the SnO_2 and La-doped SnO_2 (Wang and Liu, 2009). This value is in good agreement with the values reported by other authors on semiconductor metal oxide sensor. Figure 6 also shows that pure SnO_2 achieved better regression than La-doped SnO_2. This might due to the slight change in sensitivity stability caused by the less ordered structure of La-doped SnO_2.

Sensor response and recovery time: In order to obtain the response time, our sensor was first maintained at optimal operating temperature which is 300°C in the testing chamber under purified air atmosphere. 1500 ppm of ethanol vapour was introduced to the chamber for 50 sec once stable signal was reached. The time taken by the sensor element to achieve 90% of stable output when the gas was introduced was considered as response time. For measuring the recovery time, the sample was exposed to air again by keeping it at optimal temperature and the time taken by the sensor to reach to 90% of its original value was taken as recovery time.

Table 4: Response and recovery time for pure and La-doped SnO_2 sensors

Time	Pure SnO_2	5 at.% La	10 at.% La
Response time (sec)	22.8	26.9	35.2
Recovery time (min)	4.1	9.9	11.6

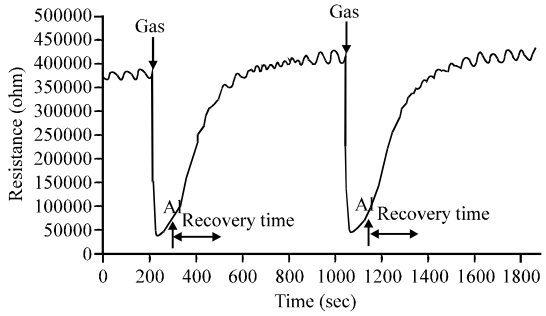

Fig. 7: Response transients for pure SnO_2 sensors (response and recovery time)

The response transients for pure and lanthanum doped SnO_2 sensor are shown in Fig. 7, the response transient for La-doped SnO_2 sensors behaved the same as that of pure SnO_2 sensor. It is evident that when the target ethanol vapour had been inserted to the detection chamber, the resistance is descending until the final resistance value for the sensors. A summary of the response and recovery time is displayed in Table 4, the response times for ethanol exposure range from 22 to 40 sec for pure SnO_2 and La-doped SnO_2 sensors. The recovery times from ethanol range from 4.1 to 11.6 min for the SnO_2 and La-doped SnO_2. From Table 4, it can be observed that pure SnO_2 sensor gives the fastest response and recovery time. The values decrease with the increase of La concentration doping on the SnO_2 sensor. The slower response time implies the decrease of chemical reaction rate that may arise due to the amount of the adsorbed O^- species decreases as part of the surface of SnO_2 is covered by the La_2O_3 and the reaction become slower. Other than that, the La_2O_3 may elevate the activation energy of the chemical reaction which will prolong the response and recovery time (Shi *et al*., 2009). In order to decrease the response and recovery time of the SnO_2 based gas sensor, other metal oxide dopant such as the noble metal Pt and Pd which possible to reduce the activation energy of the reaction can be carried out in the future. Besides, the sensors exhibited fast response when ethanol gas was introduced but took a longer time to recover to its initial value. This might be due to the existence of more end products produced from Eq. 7 which barricades the adsorption of oxygen on the sensor surface.

CONCLUSION

The present study focused on development of La-doped SnO_2 based catalytic pellet sensor by sol-gel method for detection of ethanol vapour. The experimental results indicated that 10 at.% La-doped SnO_2 sensor exhibited the highest sensitivity with optimal operating temperature of 300°C. Besides that, the sensitivity of the sensors increases linearly with the increase of ethanol concentration. However, lanthanum doping increases the response and recovery time. In order to improve the performance, it's recommended to optimize the fabrication parameters such as calcination temperature and metal loading with the sensitivity, response and recovery time in the future works. In conclusion, high sensitivity is observed in this investigation, suggesting that La-doped SnO_2 sensor is a good candidate for fabricating of ethanol gas sensor.

ACKNOWLEDGMENTS

The authors are thankful to the Malaysian Ministry of Science, Technology and Innovation (MOSTI) for providing the Long-term Science Fund (6013303) research grant. The authors are also grateful to University of Science, Malaysia for the supports provided in term of facilities and financial assistance (USM Fellowship).

REFERENCES

Caihong, W., X. Chu and M. Wu, 2007. Highly sensitive gas sensors based on hollow SnO_2 spheres prepared by carbon sphere template method. Sensors Actuators B Chem., 120: 508-513.

Chang, J.F., H.H. Kuo, I.C. Leu and M.H. Hon, 2002. The effects of thickness and operation temperature on ZnO:Al thin film CO gas sensor. Sensors Actuators B Chem., 84: 258-264.

Fang, L.M., X.T. Zu, Z.J. Li, S. Zhu, C.M. Liu, W.L. Zhou and L.M. Wang, 2008. Synthesis and characteristics of Fe^{3+}-doped SnO_2 nanoparticles via Sol-Gel-Calcination or Sol-Gel-Hydrothermal route. J. Alloys Compounds, 454: 261-267.

Ge, J.P., J. Wang, H.X. Zhang, X. Wang, Q. Pengand Y.D. Li, 2006. High ethanol sensitive SnO_2 microsphere. Sensors Actuators B Chem., 113: 937-943.

Hieu, N.V., H.R. Kim, B.K. Ju and J.H. Lee, 2008. Enhanced performance of SnO2 nanowires ethanol sensor by functionalizing with La_2O_3. Sensors Actuators B Chem., 133: 228-234.

Hyodo, T., S. Abe, Y. Shimizu and M. Egashira, 2003. Gas-sensing properties of ordered mesoporous SnO_2 and effects of coatings thereof. Sensors Actuators B Chem., 93: 590-600.

Jinkawa, T., G. Sakai, J. Tamaki, N. Miura and N. Yamazoe, 2000. Relationship between ethanol gas sensitivity and surface catalytic property of tin oxide sensors modified with acidic or basic oxides. J. Mol. Catal. A Chem., 155: 193-200.

Kapse, V.D., S.A. Ghosh, G.N. Chaudhari, F.C. Raghuwanshi and D.D. Gulwade, 2009. H_2S sensing properties of La-doped nanocrystalline In_2O_3. Vacuum, 83: 346-352.

Khodadadi, A., S.S. Mohajerzadeh, Y. Mortazavi and A.M. Miri, 2001. Cerium oxide/SnO_2-based semiconductor gas sensors with improved sensitivity to CO. Sensors Actuators B Chem., 80: 267-271.

Labidi, A., E. Gillet, R. Delamare, M. Maaref and K. Aguir, 2006. Ethanol and ozone sensing characteristics of WO_3 based sensors activated by Au and Pd. Sensors Actuators B Chem., 120: 338-345.

Lee, D.S., S. do Han, S.M. Lee, J.S. Huh and D.D. Lee, 2000. The TiO_2-adding effects in WO_3-based NO_2 sensors prepared by coprecipitation and precipitation method. Sensors Actuators B Chem., 65: 331-335.

Lou, X., C. Peng, X. Wang and W. Chu, 2007. Gas-sensing properties of nanostructured SnO_2-based sensor synthesized with different methods. Vacuum, 81: 883-889.

Mardare, D., N. Iftimie and D. Luca, 2008. TiO_2 thin films as sensing gas materials. J. Non-Crystalline Solids, 354: 4396-4400.

Rani, S., S.C. Roy and M.C. Bhatnagar, 2007. Effect of Fe doping on the gas sensing properties of nano-crystalline SnO_2 thin films. Sensors Actuators B Chem., 122: 204-210.

Rella, R., A. Serra, P. Siciliano, L. Vasanelli, G. De and A. Licciulli, 1997. CO sensing properties of SnO_2 thin films prepared by the sol-gel process. Thin Solid Films, 304: 339-343.

Ruis, A.M., A. Cornet and J.R. Morante, 2004. Study of La and Cu influence on the growth inhibition and phase transformation of nano-TiO_2 used for gas sensors. Sensors Actuators B Chem., 100: 256-260.

Shi, S., Y. Liu, Y. Chen, J. Zhang, Y. Wang and T. Wang, 2009. Ultrahigh ethanol response of SnO_2 nanorods at low working temperature arising from La_2O_3 loading. Sensors Actuators B Chem., 140: 426-431.

Stambolova, I., K. Konstantinov, S. Vassilev, P. Peshev and T. Tsacheva, 2000. Lanthanum doped SnO_2 and ZnO thin films sensitive to ethanol and humidity. Mater. Chem. Phys., 63: 104-108.

Wang, H.C., Y. Li and M.J. Yang, 2006. Fast response thin film SnO_2 gas sensors operating at room temperature. Sensors Actuators B Chem., 119: 380-383.

Wang, Z. and L. Liu, 2009. Synthesis and ethanol sensing properties of Fe-doped SnO_2 nanofibers. Mater. Lett., 63: 917-919.

Weber, I.T., A. Valentini, L.F.D. Probst, E. Longo and E.R. Leite, 2008. Catalytic activity of nanometric pure and rare earth-doped SnO_2 samples. Mater. Lett., 62: 1677-1680.

Zhu, B.L., C.S. Xie, W.Y. Wang, K.J. Huang and J.H. Hu, 2004. Improvement in gas sensitivity of ZnO thick film to volatile organic compounds (VOCs) by adding TiO_2. Mater. Lett., 58: 624-629.

Zhu, B.L., C.S. Xie, J. Wu, D.W. Zeng, A.H. Wang and X.Z. Zhao, 2006. Influence of Sb in and Bi dopants on the response of ZnO thick films to VOCs. Mater. Chem. Phys., 96: 459-465.